Analysis of the 2016 data

Alexander Aksentyev

December 13, 2016

1 Overview

In the 2016 experiment the polarized proton beam was scattered on the polarized deuterium target. The beam was cooled using electron cooling, and bunched using the COSY RF bunching system. The intensity of the cooling electron beam was 120 mA at injection, and 45 mA during acceleration. Before a cycle, the beam was stacked for 100 seconds (EXP2 $\times$ 5).

The cycles lasted thirteen minutes (792 seconds). In the first half of the cycle the target was turned on, in the second off. The target's spin state remained constant throughout, the beam's alternated through the spin up, down, and null states. In total, there were twelve cycles for each beam spin state.

The cycles are shown in Figure 1; the slopes estimated from those cycles are plotted against time in Figure 2; the slopes' summary statistics (only for the target spin state #1) are aggregated in Table 1.

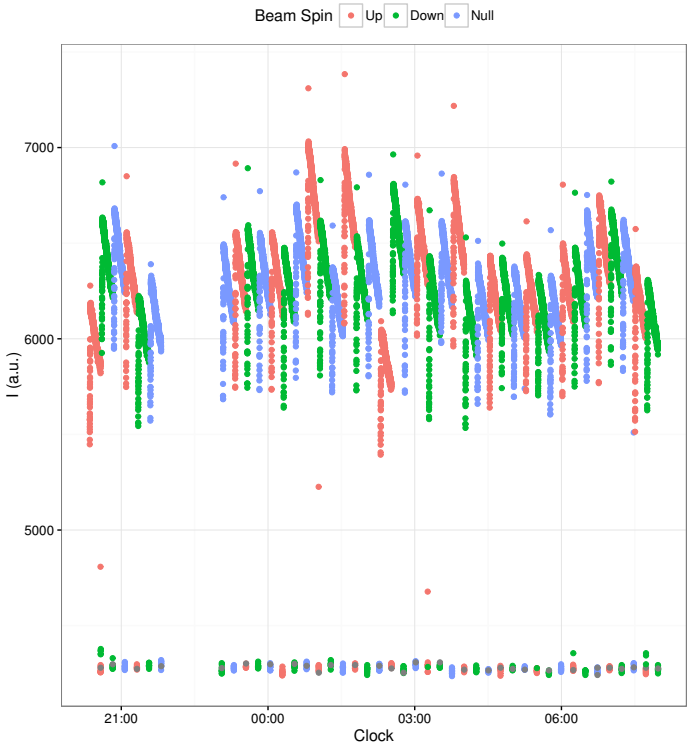

Figure 1: Cycles in 2016 colored according to the beam spin state. Before 22:30 the target spin state is 3, after it is 1.

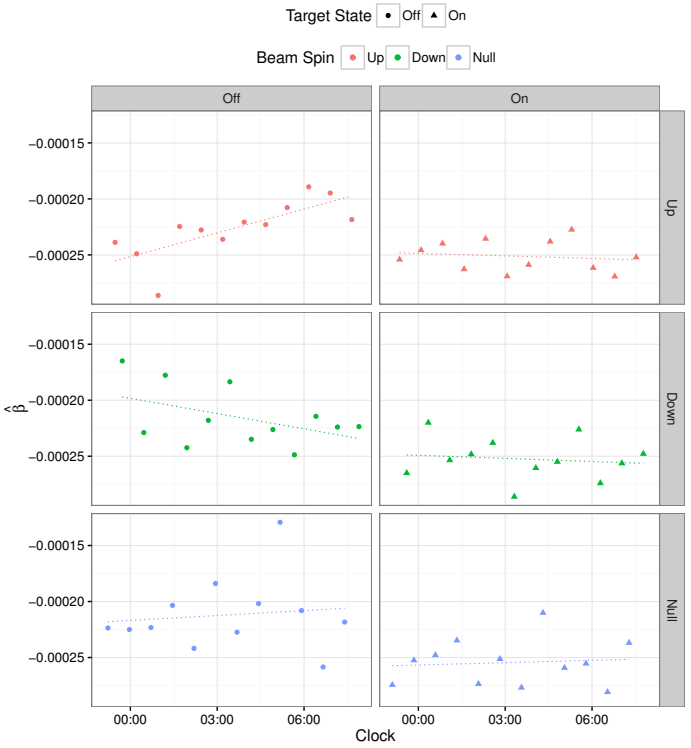

Figure 2: Slope estimates against time for the target spin state 1.

2 Properties of the data

The slopes summarized in Table 1 were obtained using Ordinary Least Squares regression. The Gauss-Markov theorem puts certain conditions on the data in order that the least squares slope estimator be minimum-variance mean-unbiased. Those conditions are: [1]

Table 1: Slope summary statistics.

Target	Spin	#	Mean (a.u.)	SE (a.u.)
Off	Up	12	$-2.26 \cdot 10^{-4}$	$7 \cdot 10^{-6}$
	Down	12	$-2.16 \cdot 10^{-4}$	$8 \cdot 10^{-6}$
	Null	12	$-2.12 \cdot 10^{-4}$	$9 \cdot 10^{-6}$
On	Up	12	$-2.51 \cdot 10^{-4}$	$4 \cdot 10^{-6}$
	Down	12	$-2.53 \cdot 10^{-4}$	$5 \cdot 10^{-6}$
	Null	12	$-2.54 \cdot 10^{-4}$	$6 \cdot 10^{-6}$

1. Linearity and additivity of the relationship;
2. Independence of the predictor and error variables (strict exogeneity);
3. No serial correlation of the error;
4. Constant variance of the error (homoskedasticity).

The Breusch-Pagan test against heteroskedasticity suggests that our data are homoskedastic; however, the Durbin-Watson test for autocorrelation of the residuals (whose statistic is the value of the auto-correlation function at lag 1) yields the lag-1 autocorrelation around 60% for all cycles (see Figure 3). [1] Autocorrelation does not affect the slope estimate itself, but in its presence the OLS estimate of its standard error is biased. To correct for that, we use a robust standard error estimator provided by the *sandwich* package of R. [2] The robust estimator takes care of both the (possible) heteroskedasticity, and the autocorrelation.

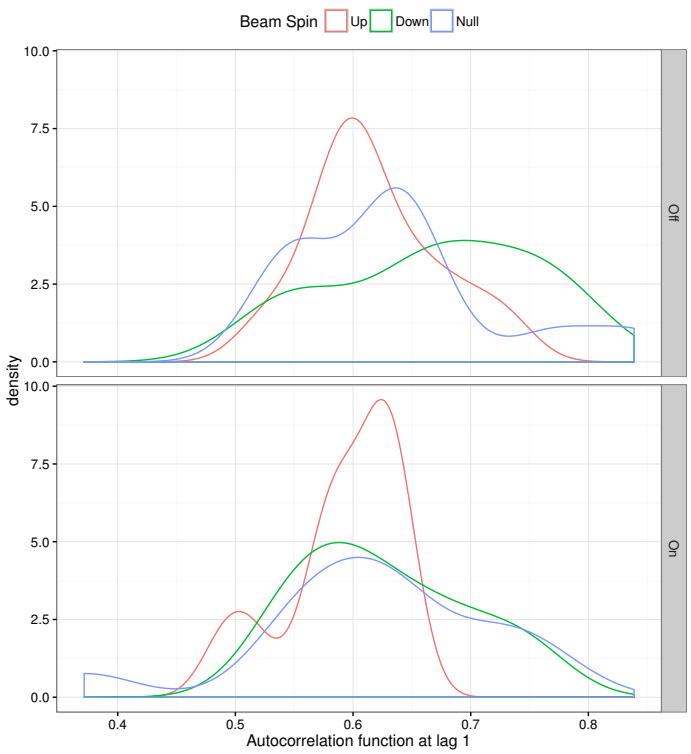

Figure 3: Distribution of the auto-correlation of the residuals at lag 1.

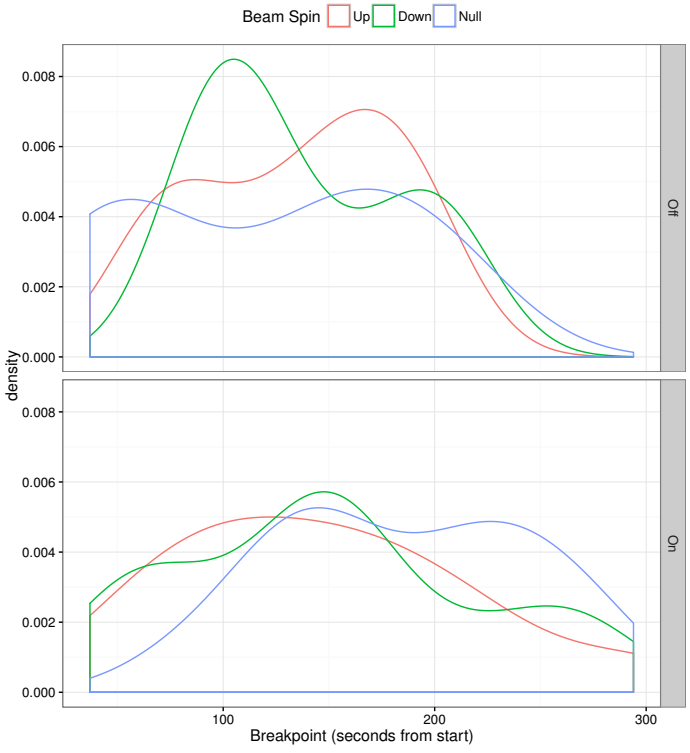

Figure 4: Point of change in the slope as found by the moving Chow test. The target-less cycles' distribution is in the upper panel.

The moving Chow test, as well as other structural tests from the package [3] suggest changes in the slope, i.e. the appropriateness of a piece-wise linear regression. The distribution of the breakpoints, as found by the Chow test, are plotted in Figure 4. One can also observe from the plot of model residuals against the fitted values (Figure 5) that the simple linear model is not appropriate for the data. One possible explanation for this behavior is the change in the pumping speed at low pressure. This effect has never been analyzed, but it could be a major practical source of systematic error.

[1] The use of the generalized least squares model with the AR1-correlated error term did not improve the fit according to both the Akaike's and Bayesian information criteria.

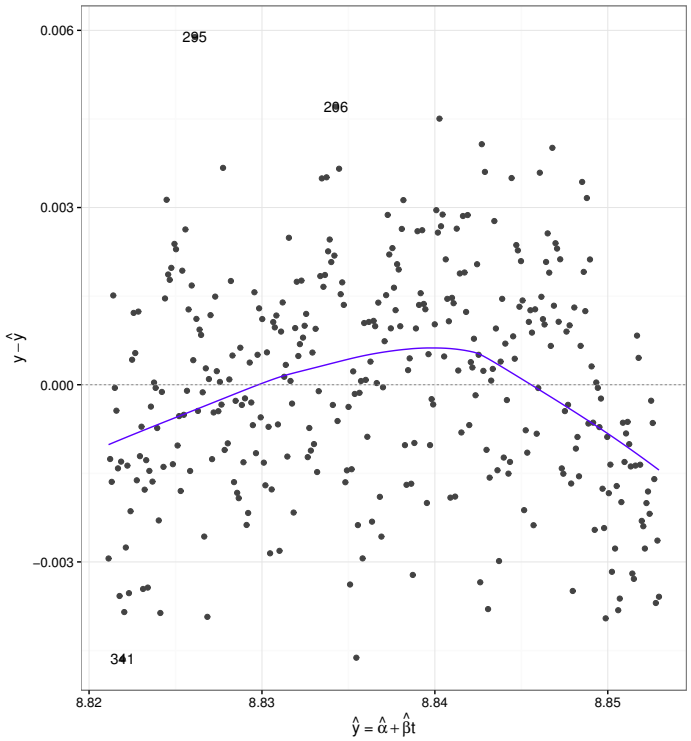

Figure 5: Plot of the linear model residuals vs. the fitted values for the target-on part of a cycle. The shape of the plot (flipped-over U) indicates that the model systematically overestimates the beam current at higher values, then underestimates in the mid range, and overestimates again at lower values.

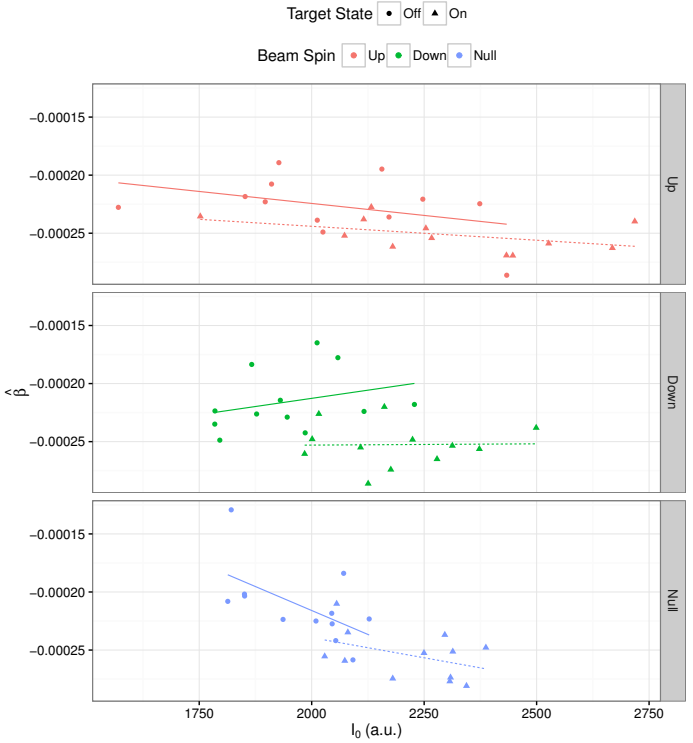

Figure 6: Slope estimates against the initial beam current. The beam current is estimated from the regression model.

Figure 6 shows that there is a dependency between the beam's life time and its intensity. The initial beam intensity I_0 was estimated as the exponentiated intercept of the linear model $\ln I_t = \ln I_0 + \beta \cdot t + \epsilon_t$, and the life time estimate is $\hat{\tau} = -1/\hat{\beta}$.

3 Obtainable estimates

The slopes we estimate are presumed to have the following, most general, form:

$$\beta = -\nu \left[\sigma_0 \left(1 + A_{y,y} P_y^t P_y\right) \Theta + \sigma_X \Theta_X\right], \tag{1}$$

where ν is the beam revolution frequency, σ_0 is the unpolarized cross section, $A_{y,y}$ is the asymmetry, P_y^t and P_y are the vertical components of respectively the target and beam polarization vectors, $\Theta = \rho d$ [cm^{-2}] is the target thickness, and $\sigma_X \Theta_X$ refers to the extra-target loss.

In principle, we can estimate both the unpolarized cross section and the asymmetry from the data we have. If we take the difference between two null beam spin state slopes ($P_y = 0$), [2] one from a target-off cycle, the other target-on,

$$\beta^0_{off} - \beta^0_{on} = \nu\sigma_0 \left(\Theta_{on} - \Theta_{off}\right),$$

from which we can estimate σ_0, once we know the target thicknesses.

The asymmetry is estimated by taking the difference between two target-on slopes with opposite beam polarizations as in

$$\beta^-_{on} - \beta^+_{on} = \nu\sigma_0 \Theta_{on} P^t (P^+ - P^-) A_{y,y}.$$

3.1 Cross section

We used the thicknesses estimated from the shift of the Schottky spectrum [4] ($\Theta_{on} = 1.1 \cdot 10^{14}$ [cm^{-2}], and $\Theta_{off} = 0$ [cm^{-2}]). The cross section estimates we got are presented in Figure 7 and Table 2. Those estimates that are based on slopes that

[2] This is done in order to remove the dependency on the unknown value of $A_{y,y}$.

are considered outliers according to Tukey's range test are labeled unsound, and those whose slopes are separated by more that 40 minutes are considered far removed. The latter classification was introduced in connection with the concern that the environmental conditions systematically changed over time.

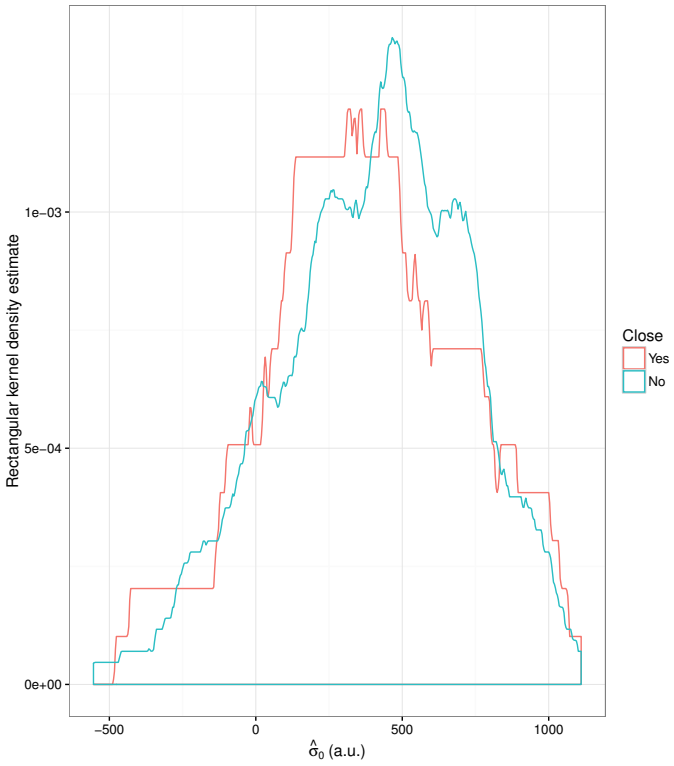

Figure 7: Rectangular kernel density estimate of cross section.

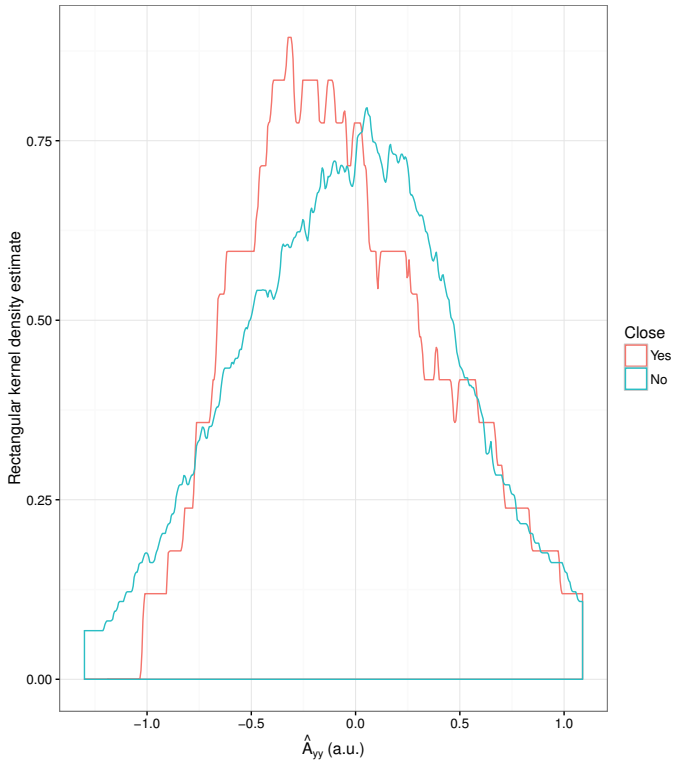

Figure 8: Kernel density estimate of $A_{y,y}$.

Table 2: Cross section summary statistics

Sound	Close	#	Mean[a](a.u.)	SE[b](a.u.)	χ^2_{red}	SE[c](a.u.)	Mode[d](a.u.)
	Yes	21	366	73	6.5	178	386
Yes	No	111	397	30	7.0	80	403
	All	132	393	28	6.9	73	400
	Yes	2	1469	22	0.1	5	1467
No	No	10	1440	83	4.2	169	1429
	All	12	1444	69	3.4	127	1435

[a] Variance weighted mean.
[b] The distribution's standard deviation divided by the square root of the sample size.
[c] According to the formula, correcting for dispersion via the χ^2_{red}.
[d] Most frequent value.

3.2 Asymmetry

The summary statistics for the asymmetry are presented in Table 3; its density estimate in Figure 8.

Table 3: Asymmetry summary statistics

Sound	Close	#	$\hat{\sigma}_0$ (a.u.)	Mean[a](a.u.)	SE[b](a.u.)	χ^2_{red}	SE[c](a.u.)	Mode[d](a.u.)
	Yes	23	366	$2.0 \cdot 10^{-2}$	$9.1 \cdot 10^{-2}$	5.8	0.23	$-4.2 \cdot 10^{-2}$
Yes	No	121	397	$2.2 \cdot 10^{-2}$	$4.6 \cdot 10^{-2}$	8.2	0.13	$-3.0 \cdot 10^{-2}$
	All	144	–	$2.2 \cdot 10^{-2}$	$4.2 \cdot 10^{-2}$	7.8	0.12	$-3.1 \cdot 10^{-2}$

[a] Variance weighted mean.
[b] The distribution's standard deviation divided by the square root of the sample size.
[c] According to the formula, correcting for dispersion via the χ^2_{red}.
[d] Most frequent value.

4 Conclusion

Data analysis revealed possible systematic effects that were never accounted for before; specifically, the possibility that the change in the pumping speed could have a significant enough effect to render the linear model inapplicable.

Other than that, the serial correlation of the error at around 60% is certainly a concern; one possible explanation for this is the feedback loop between the beam current and the current transformer, especially considering that there's a statistically significant correlation between the beam current and the slope estimate (Figure 6).

The most likely explanation for the behavior observed in Figure 2, in this author's opinion, is depolarization of the beam. This is because the target-off slopes exhibit a greater tendency to drift with time, and also because of the character of the drift. The spin-up slopes become less negative, while the spin-down slopes become more negative, and the null slopes remain more or less the same (although more dispersed). If it was simply due to the growth of the accelerator ring thickness, both type slopes would've gone more negative, which they don't. And the null slopes would be affected as well. However, the depolarization hypothesis explains why only the polarized slopes are affected, and why they tend to the less pronounced state.

This drift is the major reason why the $\hat{A}_{y,y}$ distribution has a standard deviation that's three times as big as it should be statistically, and would also explain why the distribution has a zero mean.

References

[1] D.S.G. Pollock. "Topics in Econometrics."

[2] `https://cran.r-project.org/web/packages/sandwich/sandwich.pdf`

[3] `https://cran.r-project.org/web/packages/strucchange/strucchange.pdf`

[4] H. J. Stein, M. Hartmann, I. Keshelashvili, et al. "Determination of target thickness and luminosity from beam energy losses."